Chalcogenide Letters Vol. 18, No. 5, May 2021, p. 245 - 253

Energy bandgap studies on copper chalcogenide semiconductor nanostructures using cohesive energy

M. I. Ahamed[a,*], M. Ahamed[b], A. Sivaranjani[c], S. Chockalingam[d]
[a]*Department of Electronics and Communication Engineering, E.G.S. Pillay Engineering College, Nagapattinam – 611002, Tamilnadu, India*
[b]*Bimberg Chinese-Germen Centre for Green Photonics of the Chinese Academy of Science at Changchun Institute of Optics, Fine Mechanics and Physics, Changchun- 130033, People's Republic of China*
[c]*Department of Micro-Nano Mechanical Science & Engineering, Graduate School of Engineering, Nagoya University, Nagoya 464-8603, Japan*
[d]*Department of Mechanical Engineering, E.G.S. Pillay Engineering College, Nagapattinam – 611002, Tamilnadu, India*

Investigating the properties of semiconductor nanomaterials to understand the specific behavior of nano-scale materials and predicts novel advancement of functionalized semiconductor materials that are influenced by cohesive energy. Cohesive energy is strongly associated with semiconductor nanomaterials as the energy increment by the arrangement of atoms in a crystal which is one of the most fundamental properties. In this communication, the shape and size dependence over the energy bandgap of copper chalcogenide semiconductor nanomaterials is investigated. The theoretical model is derived on cohesive energy of semiconductor nanomaterials was equated with the bulk materials. For this research, we considered Cu_2SnS_3, Cu_2SnSe_3, Cu_2SnTe_3, Cu_3SbSe_4, and $CuSbS_2$ chalcogenide matters to the study of shape and size dependent-energy bandgap. The model forecasts that the energy bandgap is inversely proportional to the size of the semiconductor. The present modeling results are correlated with established experimental data and underpin the model reported.

(Received March 13, 2021; Accepted May 6, 2021)

Keywords: Cohesive energy, Chalcogenides, Copper quantum dots, Energy bandgap

1. Introduction

In recent years, the idiosyncratic properties of semiconductor nanostructures have attracted high attention amongst researchers. The chemical and physical properties of semiconductor nanostructures fairly differ from those of bulk structures and significantly depend on size [1-4]. Semiconductor nanostructures have provided very interesting research related to optical and electronic device applications as well as to fundamental physical science. Recently Irshad et al. [5, 6] reported that electronic and optical properties of Cu_2SnS_3 and $PbSe_xS_{1-x}$ QDs ($0 \leq x \leq 1$) are determined by using Brus and Vegard's law. Notably, the surface-volume ratio of semiconductor nanocrystals is significant to analyze their properties. One of the significant properties of semiconductors is energy bandgap which plays a vital part in the optical and electronic properties of the semiconductor. Therefore it's important to study the energy bandgap variation of semiconductor nanostructures to understand the better opportunity.

Due to the wide energy bandgap, semiconductor nanostructures have extensive applications in solar cells and other optoelectronic devices. Bulk semiconductors such as silicon and germanium are limited in the optoelectronics applications due to small and indirect energy bandgap whereas silicon-based nano-photonics devices have been commercialized. Several kinds of literature reported on size-dependent energy bandgap of low dimensional structures have been reported. The size dependent's effect on energy bandgaps over one-dimensional nanostructures is

* Corresponding author: irshad_bcet@yahoo.co.in

determined under investigation on photoluminescence spectra and corresponding experimental results for InAs QDs and predictions of various theoretical models [7].

Sharma et.al reports that simple electronic structure simulations are used to analyze the shape and size-related properties of copper nanostructure which may offer a technique of tuning the energy bandgap around quantized confinement. Ascribed to the effect of quantum confinement the movement of holes and electrons in nanosized semiconductors is limited. Thus the energy difference on either side of empty states and the filled states widens the energy bandgap of the semiconductor resulting in energy levels [8].

The wider energy bandgap notably transforms the optical and electronic traits of semiconductor nanostructures in optoelectronic devices. Several works have been reported about the analyzes of the energy bandgap using photoluminescence, ultraviolet-near infrared, and X-ray photoemission spectroscopies [9-11]. However, the theoretical projection for the energy bandgap of nanostructures holds importance for understanding and realizing an application. Several theoretical models being proposed but there is still room to accommodate for the better perusal of the size-shape dependence energy bandgap of semiconductors nanostructures, which holds high importance to calculate the energy bandgap to the fullest of free approximation.

Cohesive energy is strongly affixed exclusive properties of semiconductor nanostructures [12-14]. This work presents, a theoretical model based on cohesive energy of size-shape overreliance on energy bandgap of semiconductor nanostructures. The speculative prediction is applied to the compound semiconductor nanomaterials such as Cu_2SnS_3, Cu_2SnSe_3, Cu_2SnTe_3, and Cu_3SbSe_4 with spherical and nanofilm shapes. The variation of the energy bandgap of the nanomaterials is achieved by tuning the size-shape of the semiconductor nanostructured materials. The predicted results are equated with experimental data. Further, this model is applicable even without any experimental results.

2. Theoretical framework

The Energy required to disintegrate constituent molecules by fracturing interlinked bonds is defined as Cohesive Energy. The total cohesive energy of the nanomaterial is defined as, the energy due to the provided by the surface and interior atoms, which is stated as given below,

$$E_{Total} = E_0 (n-N) + (1/2)\, E_0 N \tag{1}$$

where 'E_0' represents the cohesive energy of the semiconductor per-atom. 'N' represents the number of surface atoms and 'n' represents the total number of atoms of the nanostructure. Hence, (n-N) represents the overall counts of interior atoms in the nanostructure. To determine the cohesive energy per mole fraction, Eq. 1 can be rewritten as,

$$AE_{Total}/n = AE_0 (1- (N/n)) + (1/2n)\, AE_0\, N \tag{2}$$

where 'A' represents the Avogadro's number, AE_{Total}/n is the cohesive energy per mole fraction of the nanomaterial En, and AE_0 represents the cohesive energy per mole fraction of the corresponding bulk material (Eb). Correspondingly the Eq. 2 can be derived as,

$$En = Eb\, (1- (N/2n)) \tag{3}$$

It is highly agreed that both melting temperature and cohesive energy are parameters that describe the bonding strength of the materials. Further, it is reported that the melting point for any material has a linear relation to the cohesive energy [15]. Since the cohesive energy of nanostructures is the function of N/n, its melting point should be following relative analogous to Eq. 3. i.e.

$$T_{mp} = T_{mb}\, (1- N/2n) \tag{4}$$

T_{mp} – melting point of nano solid
T_{mb} – melting point of bulk solid

The Arrhenius expression for the electrical conductivity $\sigma\ (D,T)$ which depends upon the size and temperature is stated as,

$$\sigma\ (D,T) = \sigma_o \exp\ (-\ E_a\ (D) / k_B T) \tag{5}$$

where σ_o represents a pre exponential constant, k_B represents a Boltzmann constant and E_a (D) represents the size dependence activation energy for electron movement for nanomaterial, which is stated as,

$$E_a\ (D) = E_C - E_F \tag{6}$$

Here, Ec is the conduction band and E_F is the Fermi level. Assuming that the electrical conductivity is unconstrained of size and melting point, we get

$$\sigma\ (Bulk, T_{mb}) = \sigma\ (D, T_{mp}) \tag{7}$$

where T_{mp} and T_{mb} represent the melting point of nanostructure and corresponding three-dimensional material. Hence, from Eq. 4 and 5 we get,

$$\sigma\ (D)\ \exp\ (-\ E_a(D/k_B T_{mp}) = \sigma_o\ (bulk) \times \exp\ (-\ E_a(bulk)/k_B T_{mb}) \tag{8}$$

Neglecting the size effect on σ_o, we obtain $E_a(D)/E_a(bulk) = T_{mp}/T_{mb}$. Here the Fermi level is seen lying midst of the energy bandgap for most semiconductors, hence the activation energy defined as $E_a=E_g/2$, suggests the changes in activation energy are directly proportional to the changes in energy bandgap. Thus, we have a more suitable expression

$$\Delta E_g(D)/E_g(bulk) = |\Delta E_a(D)/E_a(bulk)| \tag{9}$$

Here, ΔE_g represents the difference in energy bandgap.

$$\Delta E_g(D)/E_g(bulk) = |(E_a(D) - E_a(bulk)\ )/E_a(bulk)| \tag{10}$$

$$\Delta E_g(D)/E_g(bulk) = 1-\ (T_{mp}/T_{mb}) \tag{11}$$

Using equation (4) & (11) the equation can be written as,

$$E_g\ (D) = E_g\ (bulk)\ (1+N/2n) \tag{12}$$

The merit of (N/2n) differs as it based on the shape and the size of nanomaterial. For spherical nanostructures, the implication of N/2n is 2d/D, where 'D' is the diameter of the nanosolid and 'd' is the diameter of an atom.

The volume of a spherical nanostructure with diameter D, is $\pi D^3/6$ similarly the nanostructure volume can be written as $\pi D^3/6$, where'd' represents diameter of an atoms, subsequently the total number 'n' is ratio of atom and nanostructure volume. i.e.

$$n= (\pi D^3/6)\ /\ (\pi d^3/6) \tag{13}$$

$$n = (D^3/\ d^3) \tag{14}$$

The nanostructure surface area is given as πD^2 and each atom's surface adds the exterior nanosolid is the facet area of the atom (circle's true area), i.e. $\pi d^2/4$. Overall surface atoms is the ratio between surface atom area (circle's true area) and surface area of the nanostructure. i.e.

$$\text{For quantum dots } E_g(D) = E_g(\text{bulk})\,(1+ 2d/D) \tag{15}$$

Similarly, the magnitude of N/2n for one-dimensional nanostructure (Quantum wire) and two-dimensional nanostructure (Quantum well) are 4d/3l and 2d/3h respectively, where 'l' represents the diameter of the quantum wire and 'h' represents the width of the quantum well. Putting the values of N/2n in Eq. 12, the below equation is obtained.

$$\text{For quantum wire, } E_g(l) = E_g(\text{bulk})\,(1+ 4d/3l) \tag{16}$$

$$\text{For quantum well, } E_g(h) = E_g(\text{bulk})\,(1+ 2d/3h) \tag{17}$$

In this work, we exert Eq. 15 - 17 to study the changes in energy bandgap of semiconductor nanomaterials of different sizes and shapes.

3. Results and discussion

A cohesive energy model was conceived for the study of the energy bandgap variations relating to the shape-size of the semiconductor nanomaterials. The necessary parameters which are significant in theoretical calculations are listed in Table 1. Fig.1 to 4 shows the model predictions of Eq. 15 for the size-dependent energy bandgap of Cu_2SnS_3, Cu_2SnSe_3, Cu_2SnTe_3, and Cu_3SbSe_4 QDs along with experimental results.

Table 1. Input parameters.

S.No	Semiconductor nanomaterials	Energy bandgap (eV)	Reference
1.	Cu_2SnS_3	0.91	[16,17]
2.	Cu_2SnSe_3	0.8	[16,18]
3.	Cu_2SnTe_3	1.18	[19]
4.	Cu_3SbSe_4	0.31	[16]
5.	$CuSbS_2$	1.02	[20]

The results evince a decrease in energy bandgap with an increase in the size of QDs. The overlapping energy levels or orbitals decrease the width of the energy band; hence the bandgap becomes narrower. This elucidates the higher energy bandgap in a semiconductor nanomaterial than a corresponding bulk semiconductor.

Fig. 5 presents the energy bandgap of Cu_2SnS_3 Quantum wire evaluated by Eq. 16, with experimental findings [24-27] which agrees with the proposed model. As shown in Fig. 5, the size and energy bandgap inversely proportional. The energy bandgap increases abruptly with the reduction of size 3 nm onwards.

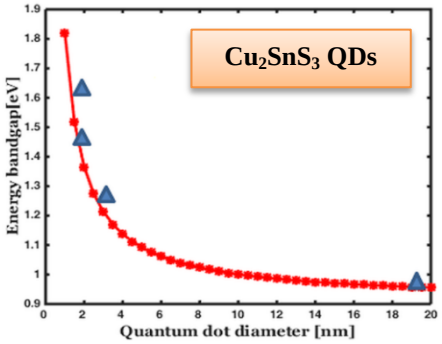

Fig. 1. Energy bandgap variation of Cu_2SnS_3 QDs with size and the experimental results are marked by solid triangle [21-23].

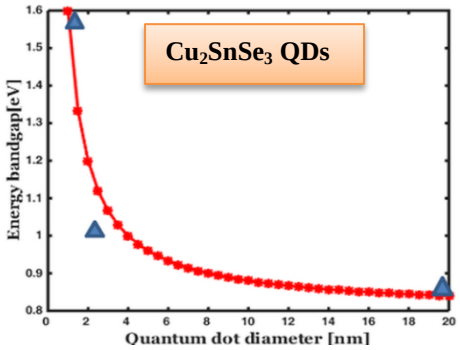

Fig. 2. Energy bandgap variation of Cu_2SnSe_3 QDs with size and the experimental results are marked by solid triangle [29-31].

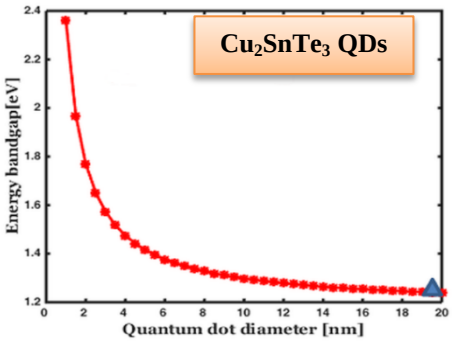

Fig. 3. Energy bandgap variation of Cu_2SnTe_3 QDs with size and the experimental results are marked by solid triangle [34].

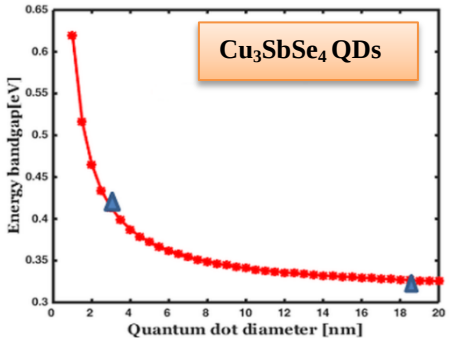

Fig. 4. Energy bandgap variation of Cu_3SbSe_4 QDs with size and the experimental results are marked by solid triangle [36, 37].

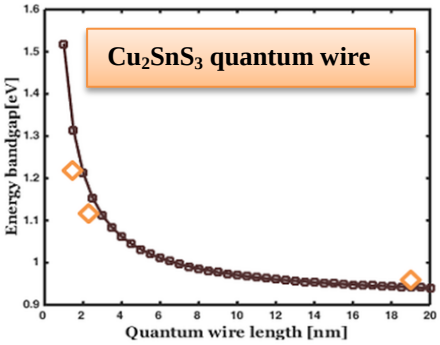

Fig. 5. Energy bandgap variation of Cu_2SnS_3 quantum wire with size and the experimental results are marked by solid diamond [24-27].

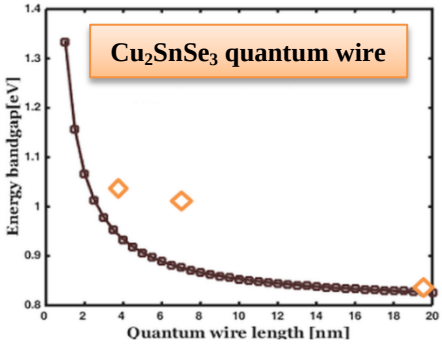

Fig. 6. Energy bandgap variation of Cu_2SnSe_3 quantum wire with size and the experimental results are marked by solid diamond [32, 33].

The size-dependent energy bandgap of Cu_2SnS_3, Cu_2SnSe_3, Cu_2SnTe_3, Cu_3SbSe_4, and $CuSbS_2$ semiconductor quantum well was calculated using Eq. 17. The results are projected in Fig. 9-12. The finding indicated that the energy bandgap of quantum well decreases with an increase in size. This tendency of decreasing energy bandgap as size increases is the same as spherical quantum dots and quantum wires. Fig. 13 shows that the effect of size decreases. This trend was speculative since the surface to volume ratio of the material increases inversely proportional to size. The experimental results were not available for the Cu_2SnSe_3, Cu_2SnTe_3, and Cu_3SbSe_4 semiconductor quantum well should be noted here.

The projected model is reported in the absence of experimental findings and it explores the vast design space for semiconductor nanomaterials which would allow researchers to engaged in

experimental work with an understanding. As per Eq. 3, cohesive energy decreases with decreasing size of quantum wells, which increases the bandgap from Eq. 17.

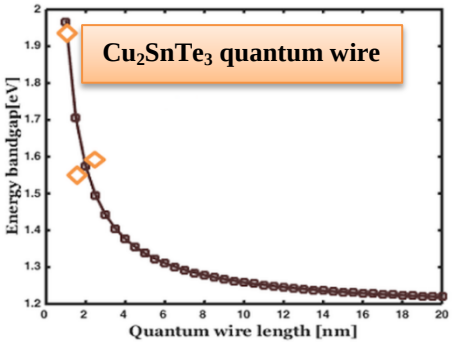

Fig. 7. Energy bandgap variation of Cu_2SnTe_3 quantum wire with size and the experimental results are marked by solid diamond [35].

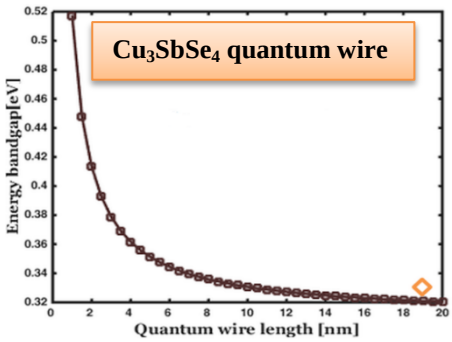

Fig. 8. Energy bandgap variation of Cu_3SbSe_4 quantum wire with size and the experimental results are marked by solid diamond [36, 37].

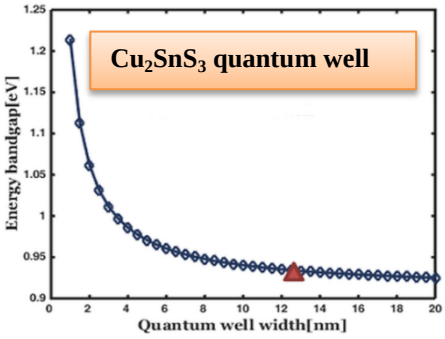

Fig. 9. Energy bandgap variation of Cu_2SnS_3 quantum well with the size and the experimental results are marked by solid triangle [28].

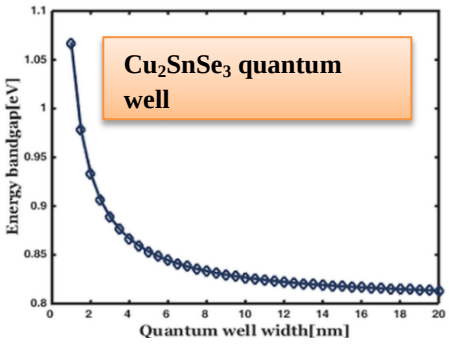

Fig. 10. Energy bandgap variation of Cu_2SnSe_3 quantum well with size.

Variation in energy bandgap for Cu_2SnSe_3 nanomaterials quantum dot and quantum wire shapes with sizes are reported in Fig. 2 and 6 along with experimental findings. Fig. 2, shows the energy bandgap as 1.6 eV when QDs radius is at 1 nm and the large energy bandgap of this compound by Eq. 16. Further, the diameter of the quantum dot slightly increases the energy bandgap tends to a gradual decrease. This prediction model assent closely with the experimental verdicts throughout the full size of Cu_2SnSe_3 quantum dots and there is good accord with the experimental work.

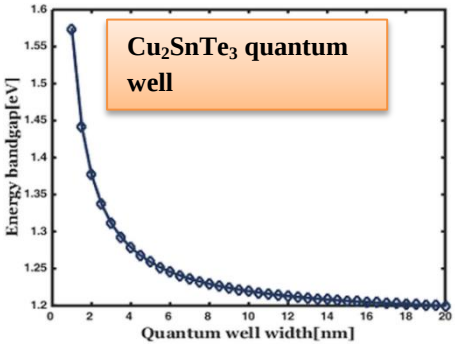

Fig. 11. Energy bandgap variation of Cu_2SnTe_3 quantum well with size.

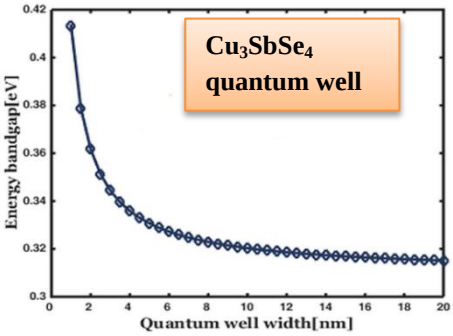

Fig. 12. Energy bandgap variation of Cu_3SbSe_4 quantum well with size.

The energy bandgap of Cu_2SnTe_3 semiconductor nanomaterial in different shapes and sizes was calculated by eq. 15 & 16. Fig. 3 & 7 show a slow decrease in the energy bandgap with an increase in the size of Cu_2SnTe_3 semiconductor nanomaterial. The predicted results comply with the existing experimental results of the Cu_2SnTe_3 nanomaterial's complete range. This ensures the correctness of the formulation used.

Fig. 4 & 8 exhibits the size dependence energy bandgap expansion of Cu_3SbSe_4 semiconductor nanomaterial along with experimental data. The energy bandgap increases rapidly with a decrease in the size of nanomaterial. Graphical representation of the decrease in energy bandgap with size confirms the existence of the quantum confinement effect in the material. But it also depends upon the shape of the QDs. The surface to volume ratio differs with shape and size according to the number of surface atoms of semiconductor nanomaterial hence influencing the cohesive energy.

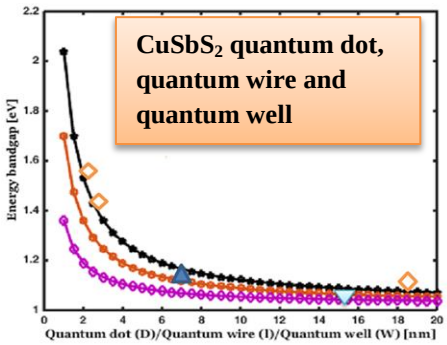

Fig. 13. Energy bandgap variation of $CuSbS_2$ quantum dot, quantum wire, and quantum well with size. The experimental findings are marked by the solid triangle and diamond [38-44].

This can be explained further, through the use of quantum mechanics. As the material reaches the nano range, the number of energy levels or orbital decreases, and the band becomes discrete to form energy levels. This causes an increase in the bandgap between the conduction band and the valence band. This represents the large energy bandgap in semiconductor nanomaterial than their corresponding bulk counterpart.

4. Conclusion

Summarizing, a straightforward theoretical model is developed to analyze the bandgap of semiconductor nanomaterials of different shapes and sizes notably, spherical quantum dots, quantum wire, quantum well. It is found from the theoretical analysis, the size-shape effects are principally caused by surface-to-volume ratio and size-dependent surface energy along with the cohesive force of semiconductor nanomaterial drops as its size reduces, which leads to increases in energy bandgap. This prediction model of energy bandgap analysis is reasonably consistent with experimental verdicts. This model will provide a significant role where experimental data are yet to be measured for many semiconductor nanomaterials.

References

[1] G. Ouyang, C. X. Wang, G. W. Yang, Chem. Rev. **109**(9), 4221 (2009).
[2] M. I. Ahamed, K. S. kumar, Mater. Sci.-Poland. **37**(2), 225 (2019).
[3] R. M. Fernando, C. F Juan, L. A Jose, V. David, F. D. A Susana, Crystals **10**(3), 226 (2020).
[4] V. G. Reshma, P. V. Mohanan, J. Lumin. **205**, 287 (2019).
[5] M. I. Ahamed, K. S. Kumar, E. E. Anand, A. Sivaranjani, J. Ovonic. Res. **16**(4), 245 (2020).

[6] M. I. Ahamed, K. S. kumar, Mater. Sci.-Poland. **37**(1), 108 (2019).
[7] F. Wang, H. Yu, S. Jeong, J. M. Pietryga, J. A. Hollingsworth, P. C. Gibbons, W. E. Buhro, ACS Nano. **2**(9), 1903 (2008).
[8] G. Sharma, S. Bahtt, R. Kumar, M. Kumar, Indian J. Pure App. Phy. **53**(7), 768 (2015).
[9] T. Torimoto, H. Kontani, Y. Shibutani, S. Kuwabata, T. Sakata, H. Mori, H. Yoneyama, J. Phys. Chem. B **105**(29) 6838 (2001).
[10] J. Nanda, B. A Kuruvilla, D. D Sarma, Phys Rev B. **59**(11), 7473 (1999).
[11] C. N. R Rao, G. U. Kulkami, P. J. Thomas, P. P. Edwards, Chem. Eur J. **8**(1), 28 (2002).
[12] X. Li, Nanotechnology **25**(18), 185702 (2014).
[13] M. Singh, S. Lara, S.Taele, J. Taibah, Univ. Sci. **11**(6), 922 (2017).
[14] M. Singh, B. M. Taele, G. Patel, Oriental J. Chem. **34**(5), 2282 (2018).
[15] W. H. Qi, Physica B: Condensed matter **368**(1-4), 46 (2005).
[16] Material properties (2020) available from World Wide Web: http://matweb.com/ accessed March, 01, 2021.
[17] L. L. Baranowski, K. Mclaughlin, P. Zawadzki, S. Lany, A. Norman, H. Hempel, R. Eichberger, T. Unold, E. Tobererand, A.S. Zakutayev, Phys. Rev. Appl. **4**(4), 044017 (2015).
[18] M. E. Norako, M. J. Greaney, R. L. Brutchey, J. Am. Chem.Soc. **134**(1), 23 (2012).
[19] W. Wang, W. Feng, T. Ding, Q. Yang, Chem. Mater. **27**(18), 6181 (2015).
[20] N. M. Alsaleh, N. Singh, U. Schwingenschlog, Phys. Rev. B **94**(12) 125440 (2016).
[21] S. Rabaoui, H. Dahman, H. B. Mansour, L. E. Mir, J. Mater. Sci.: Mater. Electron. **26**, 1119 (2015).
[22] M. Kamalanathan, H. Shamima, R. Gopalakrishnan, K. Vishista, Mat. Technol. **33**(2), 72 2017).
[23] S. Dias, K. Kumawat, S. Biswas, S. B. Krupanidhi, RSC Adv. **7**(38), 23301 (2017).
[24] D. M. Berg, R. Djemour, L. Gutay, G. Zoppi, S. Siebentritt, P. J. Dale, Thin Solid Films **520**(19), 6291 (2012).
[25] M. Nakashima, J. Fujimoto, T. Yamaguchi, M. Izaki, Appl. Phys. Express. **8**(4), 042303 (2015).
[26] D. Sandra, S. B. Krupanidhi, AIP Adv. **6**, 025217(2016).
[27] L. B. Lauryn, Z. Pawel, C. Steven, N. Dennis, L. Stephan, C. T. Adele, G. Lynn, S. David, T. William, S. T. Eric, Chem. Mater. **26**(17), 4951 (2014).
[28] N. Aihara, Y. Matsumoto, K. Tanaka, App. Phys. Lett. **108**, 092107 (2016).
[29] M. E. Norako, M. J. Greaney, R. L. Brutchey, J. Am. Chem. Soc. **134**(1), 23 (2012).
[30] J. Fan, W. C. Cabrera, L. Akselrud, I. Antonyshyn, L. Chen, Y. Grin, Inorg. Chem. **52**(19), 11067 (2013).
[31] Y. T. Zhai, S. Chen, J. H. Yang, H. J. Xiang, X. G. Gong, A. Walsh, J. Kang, S.H. Wei, Phys. Rev. B: Condens. Matter Mater. Phys. **84**(7), 0752137 (2011).
[32] G. S. Babu, Y. B. K. Kumar, Y. B. K. Reddy, V. S. Raja, Mater. Chem. Phys. **96**(2-3), 442 006).
[33] Z. Zainal A. Kassim M. Z. Hussein C. H. Ching, Mater. Lett. **58**(16), 2199 (2004).
[34] W. Wang, W. Feng, T. Ding, Q. Yang, Chem. Mater. **27**(18), 6181 (2015).
[35] J. Rakspun, A. Tubtimtae, V. Vailikhit, P. Teesetsopon, S. Choopu, J. Nanosci. Nanotechnol. **18**(6), 4204 (2018).
[36] D. Dat, S.D. Mahant, J. Phys. Chem. Solids **75**(4), 477 (2014).
[37] C. Yang, F. Huang, L. Wu, K. Xu, J. Phys. D: App. Phys. **44**(29), 295404 (2011).
[38] T. Rath, A. J. MacLachlan, M. D. Brown, S. A. Haque, J. Mater. Chem. A **3**(47), 24155 (2015).
[39] B. Yang, L. Wang, J. Han, Y. Zhou, H. Song, S. Chen, J. Zhong, L. Lv, D. Niu, J. Tang, Chem. Mater. **26**(10), 3135 (2014).
[40] D. Colombara, L. M. Peter, K. D. Rogers, J. D. Painter, S. Roncallo, Thin Solid Films **519**(21), 7438 (2011).
[41] K. Ramasamy, H. Sims, W. H. Butler, A. Gupta, Chem. Mater. **26**(9), 2891 (2014).
[42] Z. Liu, J. Huang, J. Han, T. Hong, J. Zhanga, Z. Liua, Phys. Chem. Chem. Phys. **18**(25), 16615 (2016).

[43] S. Suehiro, K. Horita, M. Yuasa, T. Tanaka, K. Fujita, Y. Ishiwata, K. Shimanoe, T. Kida, Inorg. Chem. **54**(16), 7840 (2015).
[44] S. Ikeda, S. Sogawa, Y. Tokai, W. Septina, T. Harada, M. Matsumura, RSC Adv. **4**(77), 40969 (2014).